Tetrahedron 139 (2023) 133435

Contents lists available at ScienceDirect

Tetrahedron

journal homepage: www.elsevier.com/locate/tet

A computational study of 1,3-dipolar cycloadditions of nitrile oxides with dienes

Loránd Kiss [a], Jorge Escorihuela [b, *]

[a] Institute of Organic Chemistry, Stereochemistry Research Group, Research Centre for Natural Sciences, H-1117, Budapest, Magyar Tudósok krt. 2, Hungary
[b] Departamento de Química Orgánica, Universitat de València, Avda. Vicente Andrés Estellés s/n, Burjassot, 46100, Valencia, Spain

ARTICLE INFO

Article history:
Received 27 March 2023
Received in revised form
24 April 2023
Accepted 24 April 2023
Available online 28 April 2023

Keywords:
DFT
Cycloaddition
Nitrile oxide
Diene
Reactivity
Regioselectivity
Distortion/interaction model

ABSTRACT

Density functional theory calculations at the M06-2X level of theory were employed to study the reactivity and regioselectivity of 1,3-dipolar cycloaddition reactions of nitrile oxides with cyclodienes. Calculated relative activation free energies reproduce the experimentally observed product ratios. The electronic energies of activation are found to be mainly controlled by distortion energies required to achieve the transition states. Both electronic and steric effects influence regioselectivities. Theoretical predictions were performed on previous experimental data and analyzed with the use of the distortion/interaction model. The obtained results will help in obtaining a better understanding of the factors that affect the relative cycloaddition rate.

1. Introduction

The Huisgen 1,3-dipolar cycloaddition reaction is a powerful method for constructing five-membered heterocycles [1,2]. The 1,3-dipolar cycloaddition of nitrile oxides to alkenes is a well-established methodology for the synthesis of isoxazolines [3], which constitute an important family of heterocyclic compounds with potential applications in medicinal chemistry, such as anti-influenza activities and antifungal properties [4]. Nitrile oxide 1,3-dipoles react with carbon−carbon dipolarophiles [5], such as alkenes [6], alkynes [7], and benzyne [8], to give Δ^2-isoxazolines and isoxazoles. Nitrile oxides are usually not stable dipoles; therefore, they are synthesized in situ from hydroximoyl halides, aldoximes or from primary nitroalkanes [9]. In the 1,3-dipolar cycloaddition reaction of a nitrile oxide to a terminal alkene the 5-regioisomer is formed in a regioselective manner. However, when using 1,2-disubstituted alkenes, a mixture of the 4- and 5-regioisomer is obtained [10].

Computational studies of 1,3-dipolar cycloadditions have been carried out in order to rationalize the reactivity and regioselectivity of these reactions. However, these results often contradict the experimentally observed findings. In this regard, Fukui's frontier molecular orbital (FMO) theory has been established as a powerful model for the understanding of these reactions [11]. In recent years, the conceptual density functional theory (DFT) model was developed by Parr [12] and later by Domingo [13], and the activation strain model has been developed by Houk and Bickelhaupt [14]. In these studies, parameters of various base sets have been calculated to predict and explain the regioselectivity or reactivity of these types of cycloadditions. According to most of the DFT works on 1,3-dipolar cycloaddition reactions of nitrile oxides, the concerted mechanism is preferred [15]. However, a stepwise diradical mechanism has also been proposed [16]. Despite thorough studies of 1,3-dipolar cycloaddition reactions between a nitrile oxide and an alkene and alkynes [17], results about reactions involving dienes or cyclodienes are less common.

It was shown in previous studies, that 1,3-dipolar cycloadditions of nitrile oxides with cyclodienes afforded cycloalkene-fused isoxazoline products (Scheme 1), that were later transformed into dialkenylated heterocycles via ring opening and cross metathesis [18]. The 1,3-dipolar cycloaddition with cyclopentadiene (**2**) yielded cyclopentene-fused isoxazoline derivatives in modest isolated

* Corresponding author.Departamento de Química Orgánica, Facultad de Farmacia, Universitat de Valencia, 46100, Burjassot, Valencia, Spain.
E-mail address: jorge.escorihuela@uv.es (J. Escorihuela).

https://doi.org/10.1016/j.tet.2023.133435

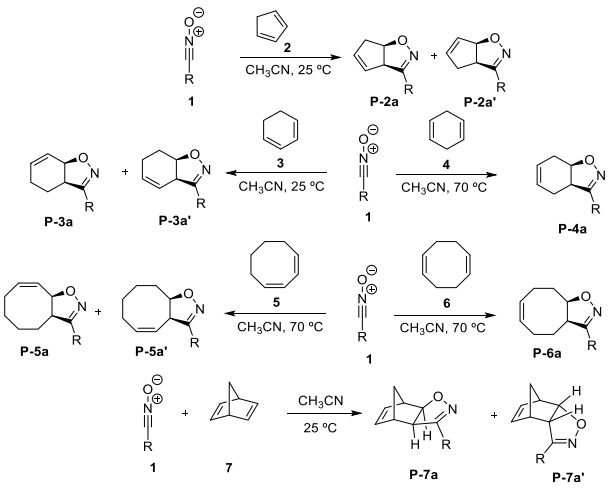

Scheme 1. 1,3-Dipolar cycloadditions of nitrile oxides with cyclodienes (R = Me, Et, Ph).

yields. When using 1,3-cyclohexadiene (**3**), the reactivity increased generating the isoxazoline derivative with a regioisomer ratio of 35:4. The transformation of 1,4-cyclohexadiene (**4**) under similar conditions only afforded traces of the desired isoxazoline product. The cycloaddition reaction of 1,3-cyclooctadiene (**5**) provided only a mixture of regioisomers of unsaturated cyclooctene-fused isoxazolines in a ratio of 2.5:1. The cycloaddition with 1,5-cyclooctadiene (**6**) at 80 °C gave a single unsaturated cycloadduct in 23% yield. The cycloaddition of nitrile oxide was extended to the constrained unsaturated bicyclic ring system containing 2,5-norbornadiene (**7**) [19], which showed an enhanced reactivity compared to the other assayed cyclodienes (**2**–**6**).

With these results in hand and with the intention of better understanding the factors that govern the reactivity and regioselectivity of 1,3-dipolar cycloaddition reactions of nitrile oxides with the cyclodienes, we decided to investigate by means of density functional theory calculations the reactivity and regioselectivity of 1,3-dipolar cycloaddition reactions of nitrile oxides with the different cyclodienes. Activation barriers were calculated by DFT calculations at the M06-2X/6-311+G(d,p) level of theory. In addition, reactivities and regioselectivities were also investigated by distortion–interaction analysis along the reaction coordinate and by frontier molecular orbital theory. The deeper understanding of 1,3-dipolar cycloaddition reactions would be of help in the design of novel isoxazoline derivatives with applications in the field of medicinal chemistry.

2. Results and discussion

Geometry optimizations were performed with Gaussian 16 [20] at the M06-2X level using the 6-311+G(d,p) basis set in acetonitrile using the SMD solvent model [21] to mimic the experimentally used solvent (acetonitrile, $\varepsilon = 37.5$). The transition structures (TS), activation energies ($\Delta E^{\ddagger}$), activation free energies ($\Delta G^{\ddagger}$), and free energies of the reaction (ΔG_{rxn}) for the different 1,3-cycloaddition reactions are shown in Fig. 1. The TS denoted as **TS-Xa** corresponds to the transition state leading to the product having the isoxazoline O-atom closer to the sp^2 *C*-atom of the cycloalkene ring, where X corresponds to cyclodiene. Meanwhile, the transition state leading to the product having the isoxazoline *C*-atom closer to the sp^2 *C*-atom of the cycloalkene ring product is denoted **TS-Xa'**. The free-energy barriers for the reactions under study using $EtNO_2$ for the generation of nitrile oxide **1a** are all around 27–32 kcal/mol. The computed trends in reactivity for these 1,3-cycloaddition reactions are identical when considering activation electronic energies or free activation energies. In particular, the free energy barriers for the reaction of cyclopentadiene (**2**) were found to be for **TS-2a** and **TS-2a'**, respectively. The difference in activation free energies ($\Delta\Delta G^{\ddagger}$) between the two both transition states is 2.3 kcal/mol, which is in good agreement with the experimental findings of complete regioselectivity favoring the product with the isoxazoline O-atom located closer to the sp^2 carbon atom of the cyclopentene ring. When evaluating the reaction of 1,3-cyclohexadiene (**3**), involving a cyclodiene with conjugated double bonds, an increase of reactivity was observed, as inferred from the calculated free energy barriers, which decreased to 29.1 kcal/mol. This lower barrier is in line with experimentally observed high conversions. The relative electronic energy ($\Delta\Delta G^{\ddagger}$) of the two regioselective transition states was slightly smaller, *i.e.,* 0.5 kcal/mol. Despite the product having the isoxazoline O-atom closer to the sp^2 *C*-atom of the cyclohexene ring was kinetically favored, the product having the isoxazoline *C*-atom closer to the sp^2 *C*-atom of the cycloalkene ring was thermodynamically favored. The reaction with 1,4-cyclohexadiene (**4**) did not proceed experimentally, and only traces of the cycloaddition product were observed [18a]. This is in agreement with the high computed barrier of 32.3 kcal/mol. For the reaction of 1,3-cyclooctadiene (**5**) and 1,5-cyclooctadiene (**6**), low yields were observed at room temperature [18a], which is in line with the similar barrier for **5** and **6** around 32 kcal/mol. A similar barrier was found when using 2,5-norbornadiene (**7**) a more strained cyclodiene. Namely, the activation free energies were found to be lower in agreement with the enhanced reactivity for this cyclodiene [18b]. DFT calculations supported the formation of the *exo*-derivative as the main product in a ratio 10 to 1, similar to the reaction of norbornadiene derivatives with cyclic nitrone derivatives [12]. This ratio corresponds to a difference in activation energies of 1.4 kcal/mol at room temperature, according to transition state theory. This is in good agreement with the calculated $\Delta\Delta G^{\ddagger}$ value (1.5 kcal/mol).

The lengths of the newly forming C···O and C···C bonds in the transition state structures are shown in Fig. 1. All 1,3-cycloadditions of dienes with nitrile oxide proceeded involving a concerted mechanism via a five-membered ring transition states [22]. A closer analysis of the transition state structures reveals that the formation of the isoxazoline derivative with the O-atom closer to the sp^2 *C*-atom of the cycloalkene ring, proceed earlier and via more favored transition states than those leading to the isoxazoline derivative with the *C*-atom closer to the sp^2 *C*-atom of the cycloalkene ring. Earlier transition states lead to less distorted geometries in the transitions state structures. All cycloadditions were found to be exergonic with free energies of reaction (ΔG_{rxn}) ranging from −25.2 to −28.7 kcal/mol for all cyclodienes under study. The 1,3-dipolar cycloaddition involving 2,5-norbornadiene proceeded with a higher exergonicity around −41 kcal/mol. Similar barriers were obtained by single point energy calculations using the hybrid wB97-D functional and the 6-311+G(2d,2p) basis set, which was utilized as a benchmark. Using this level of theory, Gibbs energy barriers were found to be 0.5–0.6 kcal/mol higher that at the M06-2X/6-311+G(d,p) level of theory but maintaining the trend in reactivity and regioselectivity.

To unravel the factors controlling the trends in reactivity of the different cyclodienes, the activation strain model, also known as the distortion/interaction model, was applied to analyze the transition states [14]. This theoretical model has been successfully applied to a wide range of chemical reactions during the past decade, including nucleophilic substitution [23], elimination [24], cycloadditions [25], organometallic chemistry [26], and other processes in organic chemistry. According to this model, the

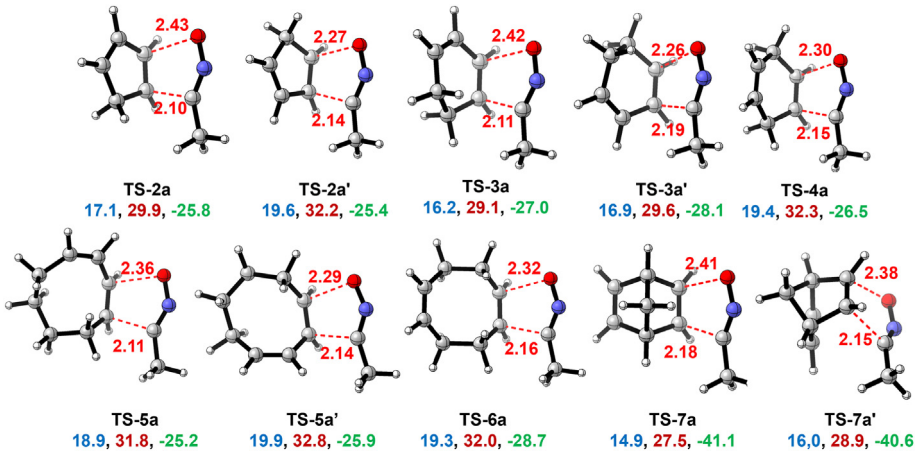

Fig. 1. Optimized structures of the transition states at the M06-2X/6-311+G(d,p) level of theory with bond forming distances in Å. Values of activation energy ($\Delta E^{\ddagger}$), activation free energy ($\Delta G^{\ddagger}$), and free energy of the reaction (ΔG_{rxn}) are shown below each structure in blue, red, and green, respectively, in kcal mol^{-1}.

transition state structure is decomposed into two fragments (dipole and dipolarophile) and the energy is separately calculated by single-point energy calculations on the distorted fragment. The difference in energy between the distorted fragment and the optimized ground-state geometry is known as the distortion energy. The difference between the activation energy ($\Delta E^{\ddagger}$) and the total distortion energy (E_{dist}) corresponds to the interaction energy (E_{int}), which is given as a negative value (*i.e.*, stabilizing) and, hence, it counteracts the distortion energy. The black arrows correspond to the activation energies ($\Delta E^{\ddagger}$). The green arrows correspond to the distortion energies of the dipolarophiles, whereas the blue arrows correspond to the distortion energies of the dipoles. The total length of blue and green arrows corresponds to the total distortion energy (E_{dist}). The red arrows correspond to the favorable interaction energies (E_{int}). The transition structures and activation energies for the different 1,3-cycloaddition reactions are shown in Fig. 2.

For all transition states involved in the 1,3-dipolar cycloaddition of nitrile oxide **1a** and the different cyclodienes (**2**–**7**), the distortion energy of nitrile oxide **1a** was found to be the main contributor to the distortion energy, which ranged from 20.1 to 24.7 kcal/mol, in line with previously reported 1,3-dipolar cycloaddition studies [27]. In the TS structures, both the O–N–C and the N–C–C angles of the distorted dipole, *i.e.*, nitrile oxide **1a**, varies from 139° to 142° and from 143° to 147°, respectively. The greater the O–N–C angle decreases, the greater the distortion and the higher the distortion energy. This deviation from linear structure in the ground-state geometry is responsible for the higher distortion energy of the dipole. In contrast, the distortion energy of the dipolarophile (cyclodiene) was relatively small and varied from 4.1 to 6.2 kcal/mol. From all cyclodienes under study, 2,5-norbornadiene (**7**) displayed the lowest distortion energy. When comparing the two TSs in the cycloaddition with cyclopentadiene (**2**), the transition state leading to the product having the isoxazoline O-atom closer to the sp^2 *C*-atom of the cycloalkene ring (**TS-2a**) displays a distortion energy 1.5 kcal/mol lower than that of **TS-2a′**, mainly attributed to the higher distortion energy arising from nitrile oxide **1a**, and a higher interaction energy. In reaction with 1,3-cyclohexadiene (**3**), the 0.7 kcal/mol difference in $\Delta E^{\ddagger}$ favoring **TS-3a** is originated from the difference in the interaction energy, as **TS-3a** and **TS-3a′**, have similar total distortion energies. The nature of the differing interaction energy for the TS leading to the two possible regioisomers can be rationalized according to the different orbital interaction, which should be more favorable in **TS-2a** and **TS-3a**, when

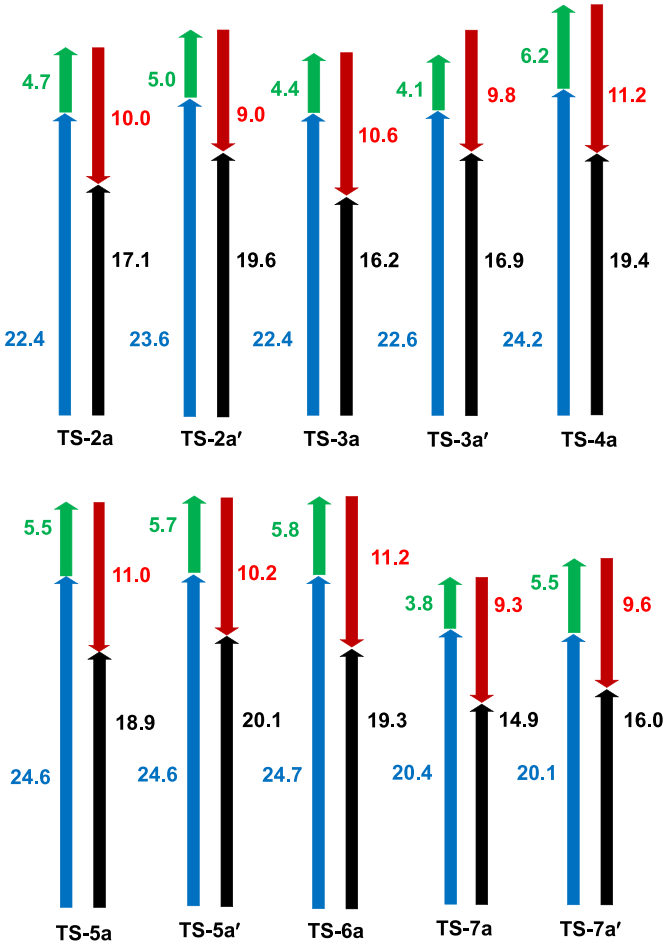

Fig. 2. Graph of distortion, interaction, and activation energies for the 1,3-dipolar cycloaddition of nitrile oxide **1a** and cyclodienes (blue: distortion energy of dipole, green: distortion energy of dipolarophile, red: interaction energy, black: activation energy). Energies are given in kcal mol^{-1}.

compared to **TS-2a′** and **TS-3a'** (see Fig. S1, Supporting Information). The reaction with 1,4-cyclohexadiene (**4**) showed a higher distortion energy compared to that of 1,3-cyclohexadiene (**3**), which should be responsible of the higher activation barrier.

Interestingly, when comparing the conjugated 1,3-cyclooctadiene (**5**) and non-conjugated 1,5-cyclooctadiene (**6**), similar distortion energies were computed. Finally, for the reaction with 2,5-norbornadiene (**7**), the difference in the activation energies can be attributed to the higher distortion energy of the dipole in the *endo* transition state (**TS-7a'**).

Given the fact that the transition states shift along the reaction coordinate - some are early (low strain) while others are late (high strain), a distortion/interaction-activation strain analysis on the reaction coordinate defined as newly forming *C*—C bond was performed for transition states involving cyclodienes **2**, **3** and **5**. Fig. 3 shows the distortion/interaction-activation strain analysis of the IRC for cycloadditions going via **TS-2a** (red), **TS-2a'** (pale red), **TS-3a** (blue), **TS-3a**′(pale blue), **TS-5a** (green) and **TS-5a'** (pale green). As shown in Fig. 3, cycloadditions leading to the formation of to the product having the isoxazoline O-atom closer to the sp^2 *C*-atom of the cycloalkene ring, *i.e.,* **TS-2a**, **TS-3a** and **TS-5a**, are characterized by an early transition state, with a relatively long forming *C*—O bond distance, in particular **TS-2a** and **TS-3a**. The approach leading to the formation of the other regioisomer via **TS-2a**′, **TS-3a**′ and **TS-5a'**, is reflected in an increase of distortion energies, now for both dipole and dipolarophiles, and a decrease in the interaction energy.

The 1,3-dipolar cycloaddition using $PhCH_2NO_2$ for the in situ generation of nitrile oxide **1b** was also studied (Fig. 4). From the experimental observations, $PhCH_2NO_2$ generally gave higher yields than $CH_3CH_2NO_2$ [18a]; thus, lower activation barriers would be expected for reactions involving this reagent as the dipole source. The transition structures (TS) and activation energies for the different 1,3-cycloaddition reactions with cyclodienes **2**—**7** leading to the product having the isoxazoline O-atom closer to the sp^2 *C*-atom of the cycloalkene ring are shown in Fig. 4. The computed activation energies ($\Delta E^{\ddagger}$) and activation free energies ($\Delta G^{\ddagger}$) were found to be lower than those for the 1,3-dipolar cycloaddition using $CH_3CH_2NO_2$, showing the higher reactivity of **1b**. Furthermore, all reactions proceed with an exergonicity (ΔG_{rxn}) higher than those computed for the reaction with **1a**. Again, the reaction of 2,5-norbornadiene (**7**) displayed the lowest activation free energy in good agreement with the enhanced reactivity for this cyclodiene.

The activation strain model was also applied to analyze the transition states of the different cyclodienes (**2**—**7**). All transition states involved in the 1,3-dipolar cycloaddition displayed nitrile oxide **1b** distorted from linear geometry in the ground state (Fig. 5). This deviation was responsible for the higher distortion energy of the nitrile oxide **1b**, which was the main contributor to the total distortion energy. In the distorted nitrile oxide **1b** from the TS structures, the O—N—C varies from 139° to 142°, whereas the N—C—C angle ranges from 143° to 145° (Fig. 5a). As observed for the 1,3-dipolar cycloaddition with nitrile oxide **1a**, the distortion energy of the dipolarophile (cyclodiene) was significantly lower and varied from 3.7 to 6.1 kcal/mol (Fig. 5b). In a similar manner, as observed for the CH_3CNO dipole, conjugated cyclodienes had the lowest total distortion energy, which would be responsible of the lower activation barriers. When comparing 1,3-cycloadditions of 1,3-cyclohexadiene (**3**) and non-conjugated 1,5-cyclohexadiene (**4**), both distortion energies of dipole and dipolarophile were higher for **TS-4b**. In the TS structures, the dipole had a more distorted structure in **TS-4b**, as the change in O—N—C angle was higher, which was reflected in a higher dipole distortion energy ($E_{dist(1b)}$). The lower activation barrier for **TS-3b** is in agreement with the experimental yield over the product coming from TS-4b. Again, the reaction with 2,5-norbornadiene (**7**) displayed the lowest activation energy, which can be attributed to the lower distortion energy of the dipole and the dipolarophile in the transition state (**TS-7b**).

To investigate the reactivity of the different cyclodienes acting as dipolarophiles, we computed the energies of the frontier molecular orbitals (FMO) of the two dipoles and the different dienes acting as dipolarophiles. By means of this theory, reaction rates have been rationalized in cycloaddition reactions [28]. The results are shown in Fig. 6. In normal-electron demand 1,3-cycloaddion reactions, the highest occupied molecular orbital (HOMO) of the dipole interacts with the lowest unoccupied molecular orbital (LUMO) of the dipolarophile. Two conclusions can be extracted from the FMO analysis. First, the HOMO of **1a** is 1.41 eV lower in energy than that of **1b**. Thus, the HOMO of **1b** interacts more

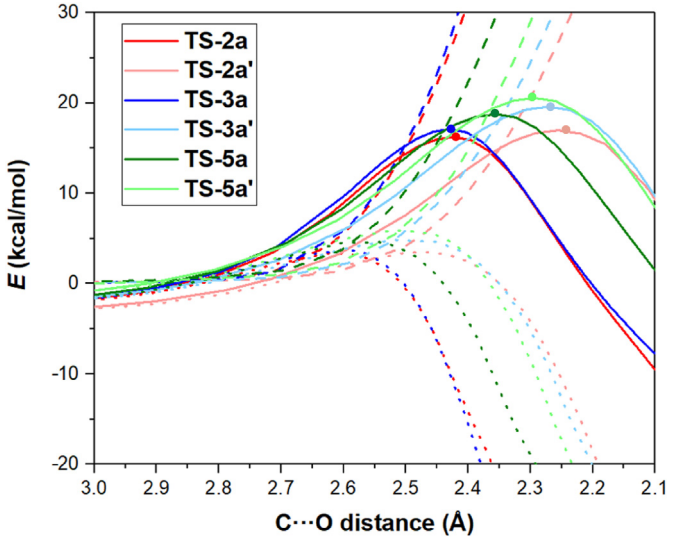

Fig. 3. Activation energy ΔE_{act}(solid), total distortion energy ΔE_{dist}(dashed), and interaction energy ΔE_{int}(dotted) along the reaction coordinate (forming C—O bond distance in angstroms) for cycloaditions of **TS-1a** with **TS-2a** (red), **TS-2a'** (pale red), **TS-3a** (blue), **TS-3a'** (pale blue), **TS-5a** (green)and **TS-5a'** (pale green).

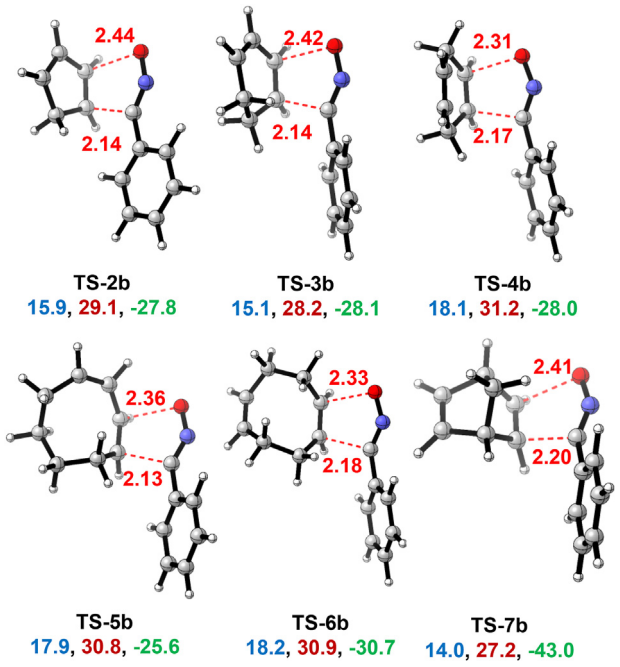

Fig. 4. Optimized structures of the transition states at the M06-2X/6-311+G(d,p) level of theory with bond forming distances in Å. Values of activation energy ($\Delta E^{\ddagger}$), activation free energy ($\Delta G^{\ddagger}$), and free energy of the reaction (ΔG_{rxn}) are shown below each structure in blue, red, and green, respectively, in kcal mol^{-1}.

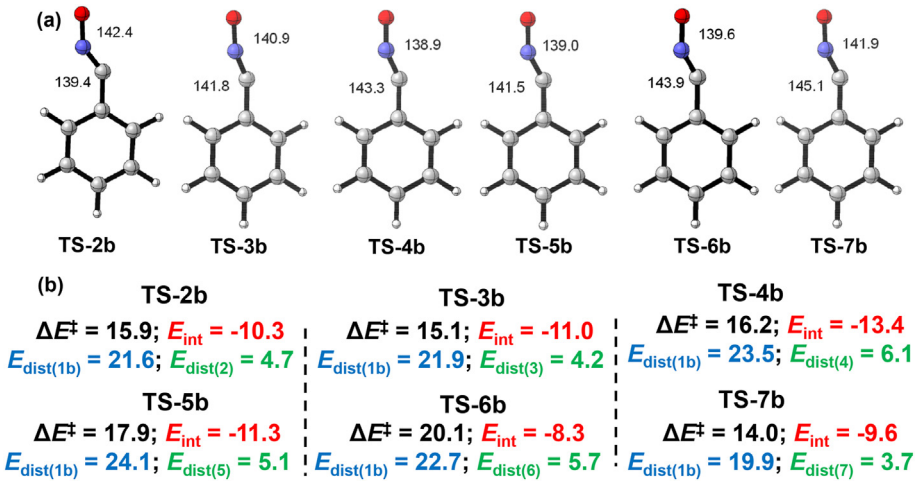

Fig. 5. (a) Distorted structures of nitrile oxide **1b** for the different transition states for the 1,3-dipolar cycloaddition of nitrile oxide **1b** and cyclodienes. (b) Values of activation energy ($\Delta E^{\ddagger}$, in black), interaction energy (E_{int}, in red), distortion energy of dipole ($E_{dist(1b)}$, in blue) and distortion energy of dipolarophile ($E_{dist(x)}$, in green) for the 1,3-dipolar cycloaddition of nitrile oxide **1b** and cyclodienes. Energies are given in kcal mol^{-1}.

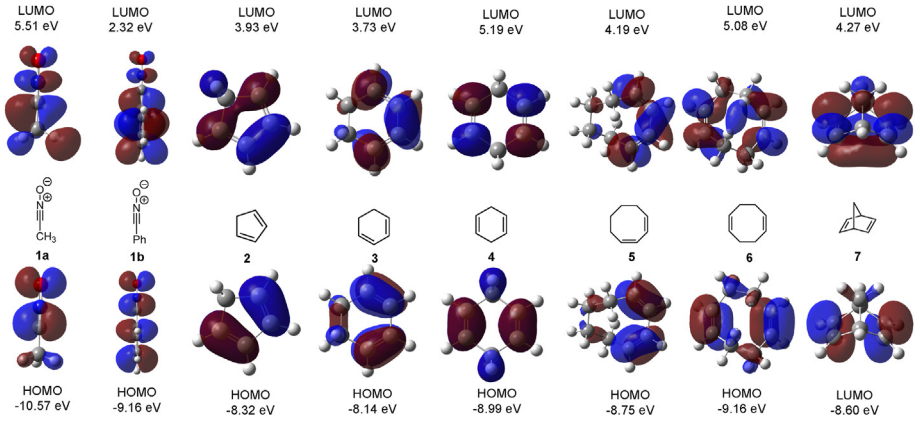

Fig. 6. Frontier molecular orbitals (FMO) involved in the 1,3-dipolar cycloaddition of nitrile oxides and dienes calculated at the HF/6-31G level of theory.

strongly with the LUMO of the dipolarophiles. As a consequence, higher interaction energies were calculated for **1b**, given the strong interaction of the low-lying LUMO with the HOMO of the dipolarophile. The LUMO of conjugated dienes is lower in energy than that of non-conjugated cyclodienes. Consequently, the HOMO of the dipole interacts more strongly with the LUMO of the dipolarophile. This is in agreement with the more favorable interaction energy for conjugated dienes **3** and **5**, in comparison to that of **4** and **6**.

3. Conclusions

The reactivity and regioselectivity of 1,3-dipolar cycloaddition reactions of nitrile oxides with cyclodienes have been investigated by means of density functional theory calculations at the M06-2X level of theory. The computed free energies of activation are in agreement with experimentally observed product ratios. The activation strain model revealed that the regioselectivity is mainly governed by the distortion energies of the nitrile oxide. When benzonitrile oxide was used instead of ethylnitrile oxide, the favorable interaction energies increase. The results found in this study will help in obtaining a better understanding of the factors that affect the relative cycloaddition rates and will pave the way for the rational design of novel 1,3-dipolar cycloaddition reactions and for the synthesis of novel isoxazoline derivatives with applications in the field of medicinal chemistry.

4. Associated content

Description of computational methods; computed energies and cartesian coordinates for all reported of the stationary points. This material is available free of charge via the Internet at http://pubs.acs.org.

Author contributions

All authors have given approval to the final version of the manuscript.

Funding sources

The authors gratefully acknowledge financial support from the National Research, Development and Innovation Office of Hungary (NKFIH/OTKA K-142266).

Declaration of competing interest

The authors declare that they have no known competing financial interests or personal relationships that could have appeared to influence the work reported in this paper.

Data availability

Data will be made available on request.

Acknowledgment

The computational resources from the Servei d'Informàtica de la Universidad de Valencia (SIUV) are gratefully acknowledged for providing access to supercomputing resources.

Appendix A. Supplementary data

Supplementary data to this article can be found online at https://doi.org/10.1016/j.tet.2023.133435.

References

[1] (a) R. Huisgen, Kinetics and mechanism of 1,3-dipolar cycloadditions, Angew. Chem., Int. Ed. 2 (1963) 633–645;
(b) R. Huisgen, 1,3-Dipolar cycloadditions. Past and future, Angew. Chem. Int. Ed. 2 (1963) 565–598.

[2] M. Breugst, H.-U. Reißig, The huisgen reaction: milestones of the 1,3-dipolar cycloaddition, Angew. Chem. Int. Ed. (59) (2020) 12293–12307.

[3] (a) P. Ghosh, S.L. Mondal, M. Baidya, Ascending of cycloaddition strategy for N–O heterocycles, Synthesis 54 (2022) 1043–1054;
(b) G. Kumar, R. Shankar, 2-Isoxazolines: a synthetic and medicinal overview, ChemMedChem 16 (2021) 430–447;
(c) A. Galbiati, A. Zana, C. Coser, L. Tamborini, N. Basilico, S. Parapini, D. Taramelli, P. Conti, Development of potent 3-Br-isoxazoline-Based antimalarial and antileishmanial compounds, ACS Med. Chem. Lett. 12 (2021) 1726–1732;
(d) K. Kaur, V. Kumar, A.K. Sharma, G.K. Gupta, Isoxazoline containing natural products as anticancer agents: a review, Eur. J. Med. Chem. 77 (2014) 121–133;
(e) B. Engels, M. Christl, What controls the reactivity of 1,3-dipolar cycloadditions? Angew. Chem. Int. Ed. 48 (2009) 7968–7970;
(f) K. Rück-Braun, T.H. Freysoldt, F. Wierschem, 1,3-Dipolar cycloaddition on solid supports: nitrone approach towards isoxazolidines and isoxazolines and subsequent transformations, Chem. Soc. Rev. 34 (2005) 507–516;
(g) S. Kobayashi, K.A. Jorgensen, Cycloaddition Reactions in Organic Synthesis, Wiley-VCH, Weiheim, 2002.

[4] (a) A.A. Fuller, B. Chen, A.R. Minter, A.K. Mapp, J. Am. Chem. Soc. 127 (2005) 5376–5383;
(b) J.W. Bode, N. Fraefel, D. Muri, E.M. Carreira, A general solution to the modular synthesis of polyketide building blocks by kanemasa hydroxy-directed nitrile oxide cycloadditions, Angew. Chem. Int. Ed. 40 (2001) 2082–2085;
(c) R.P. Tangallapally, D.S. Rakesh, N. Budha, R.E.B. Lee, A.J.M. Lenaerts, B. Meibohm, R.E. Lee, Discovery of novel isoxazolines as anti-tuberculosis agents, Bioorg. Med. Chem. Lett. 17 (2007) 6638–6642;
(d) T.M. Sielecki, J. Liu, S.A. Mousa, A.L. Racanelli, E.A. Hausner, R.R. Wexler, R.E. Olson, Synthesis and pharmacology of modified amidine isoxazoline glycoprotein IIb/IIIa receptor antagonists, Bioorg. Med. Chem. Lett. 11 (2001) 2201–2204;
(e) A.P. Kozikowski, S. Tapadar, D.N. Luchini, K.H. Kim, D.D. Billadeau, Use of the nitrile oxide cycloaddition (NOC) reaction for molecular probe generation: a new class of enzyme selective histone deacetylase inhibitors (HDACIs) showing picomolar activity at HDAC6, J. Med. Chem. 51 (2008) 4370–4373.

[5] K.B.G. Torsell, Nitrile Oxides, Nitrones and Nitronates in Organic Synthesis, VCH, New York, 2008.

[6] (a) N. Umemoto, A. Imayoshi, K. Tsubaki, Nitrile oxide cycloaddition reactions of alkenes or alkynes and nitroalkanes substituted with O-alkyloxime groups convertible to various functional groups, Tetrahedron Lett. 61 (2020), 152213;
(b) J. Plumet, 1,3-Dipolar cycloaddition reactions of nitrile oxides under "non-conventional" conditions: green solvents, irradiation, and continuous flow, ChemPlusChem 85 (2020) 2252–2271.

[7] (a) Q. Feng, H. Huang, J. Sun, Ru-catalyzed [3 + 2] cycloaddition of nitrile oxides and electron-rich alkynes with reversed regioselectivity, Org. Lett. 23 (2021) 2431–2436;
(b) S.N. Afraj, C. Nuzlia, C. Chen, G.-H. Lee, Multicomponent coupling reaction and intramolecular nitrile oxide–alkyne cycloaddition towards isoxazolo [3,4]-pyrrolizines, Asian J. Org. Chem. 5 (2016) 1015–1026;
(c) F. Heaney, Nitrile oxide/alkyne cycloadditions – a credible platform for synthesis of bioinspired molecules by metal-free molecular clicking, Eur. J. Org. Chem. 2012 (2012) 3043–3058;
(d) M.L. McIntosh, M.R. Naffziger, B.O. Ashburn, L.N. Zakharov, R.G. Carter, Highly regioselective nitrile oxide dipolar cycloadditions with *ortho*-nitrophenyl alkynes, Org. Biomol. Chem. 10 (2012) 920–9213;
(e) P. Pevarello, R. Amici, M. Colombo, M. Varasi, Nitrile oxide cycloaddition of non-activated alkynes: a novel approach to the synthesis of neuroactive isoxazoles, J. Chem. Soc., Perkin Trans. 1 (1993) 2151–2152.

[8] (a) M. Sarmaha, H. Hazarikaa, P. Gogo, Synthesis 54 (2022) 4932–4962;
(b) A.V. Dubrovskiy, N.A. Markina, R.C. Larock, Use of benzynes for the synthesis of heterocycles, Org. Biomol. Chem. 11 (2013) 191–218;
(c) C. Spiteri, S. Keeling, J.E. Moses, New synthesis of 1-substituted-1H-indazoles via 1,3-dipolar cycloaddition of in situ generated nitrile imines and benzyne, Org. Lett. 12 (2010) 3368–3371;
(d) C. Spiteri, C. Mason, F. Zhang, D.J. Ritson, P. Sharma, S. Keeling, J.E. Moses, An efficient entry to 1,2-benzisoxazoles via 1,3-dipolar cycloaddition of in situ generated nitrile oxides and benzyne, Org. Biomol. Chem. 8 (2010) 2537–2542;
(e) C. Spiteri, P. Sharma, F. Zhang, S.J.F. Macdonald, S. Keeling, J.E. Moses, An improved synthesis of 1,2-benzisoxazoles: TBAF mediated 1,3-dipolar cycloaddition of nitrile oxides and benzyne, Chem. Commun. 46 (2010) 1272–1274;
(f) A.V. Dubrovskiy, R.C. Larock, Synthesis of benzisoxazoles by the [3 + 2] cycloaddition of in situ generated nitrile oxides and arynes, Org. Lett. 12 (2010) 1180–1183.

[9] (a) T. Mukaiyama, T. Hoshino, The reactions of primary nitroparaffins with isocyanates, J. Am. Chem. Soc. 82 (1960) 5339–5342;
(b) D.P. Curran, C.J. Fenk, Thermolysis of bis[2-[(trimethylsilyl)oxy]propyl] furoxan (TOP-furoxan). The first practical method for intermolecular cycloaddition of an in situ generated nitrile oxide with 1,2-di- and trisubstituted olefins, J. Am. Chem. Soc. 107 (1985) 6023–6028;
(c) Y. Basel, A. Hassner, An improved method for preparation of nitrile oxides from nitroalkanes for in situ dipolar cycloadditions, Synthesis 1997 (1997) 309–312;
(d) L. Cecchi, F. De Sarlo, F. Machetti, Prof. D synthesis of 4,5-dihydroisoxazoles by condensation of primary nitro compounds with alkenes by using a copper/base catalytic system, Chem. Eur J. 14 (2008) 7903–7912.

[10] (a) G.B. Pipim, R. Tia, E. Adei, Computational exploration of the 1,3-dipolar cycloaddition reaction of 7-isopropylidenebenzonorbornadiene with nitrile oxide and cyclic nitrone derivatives, J. Phys. Org. Chem. 34 (2021) e4174;
(b) J.E. Moore, M.W. Davies, K.M. Goodenough, R.A.J. Wybrow, M. York, C.N. Johnson, J.P.A. Harrity, Investigation of the scope of a [3+2] cycloaddition approach to isoxazole boronic esters, Tetrahedron 61 (2005) 6707–6714.

[11] (a) S. Chen, T. Hu, K.N. Houk, Energy of concert and origins of regioselectivity for 1,3-dipolar cycloadditions of diazomethane, J. Org. Chem. 86 (2021) 6840–6846;
(b) K. Fukui, Role of frontier orbitals in chemical reactions, Science 218 (1982) 747–754;
(c) K.N. Houk, J. Sims, R.E. Duke, R.W. Strozier, J.K. George, Frontier molecular orbitals of 1,3 dipoles and dipolarophiles, J. Am. Chem. Soc. 95 (1973) 7287–7301.

[12] (a) P.K. Chattaraj, R.G. Parr, Density functional theory of chemical hardness, in: K.D. Sen, D.M.P. Mingos (Eds.), Chemical Hardness, Structure and Bonding, Springer-Verlag, Berlin, 1993;
(b) R.G. Parr, W. Yang, Density Functional Theory of Atoms and Molecules, Oxford University Press, Oxford, 1989.

[13] (a) L.R. Domingo, M. Ríos-Gutiérrez, R. Chulan, M.H.H. Mahmoud, M.M. Ibrahim, S.M. El-Bahy, L. Rhyman, P. Ramasami, Unveiling the non-polar [3+2] cycloaddition reactions of cyclic nitrones with strained alkylidene cyclopropanes within a molecular electron density theory study, RSC Adv. 12 (2022) 25354–25363;
(b) L.R. Domingo, M. Ríos-Gutiérrez, P. Pérez, A molecular electron density theory study of the enhanced reactivity of aza aromatic compounds participating in diels–alder reactions, Org. Biomol. Chem. 18 (2020) 292–304;
(c) L.R. Domingo, A new C–C bond formation model based on the quantum chemical topology of electron density, RSC Adv. 4 (2014) 32415–32428.

[14] (a) F.M. Bickelhaupt, K.N. Houk, Analyzing reaction rates with the distortion/interaction-activation strain model, Angew. Chem., Int. Ed. 56 (2017) 10070–10086;
(b) F. Liu, Y. Liang, K.N. Houk, Bioorthogonal cycloadditions: computational analysis with the distortion/interaction model and predictions of reactivities, Acc. Chem. Res. 50 (2017) 2297–2308.

[15] (a) X. Luo, S. Liu, Y. Lan, Mechanism and regioselectivity of 1,3-dipolar cycloaddition of nitrile oxides to 3-methylene oxindole: a density functional theory study, ChemistrySelect 5 (2020) 8421–8428;
(b) S. Liu, Y. Lei, X. Qi, Y. Lan, Reactivity for the diels–alder reaction of cumulenes: a distortion-interaction analysis along the reaction pathway, J. Phys. Chem. A 118 (2014) 2638–2645;
(c) Y. Lan, S.E. Wheeler, K.N. Houk, Extraordinary difference in reactivity of ozone (OOO) and sulfur dioxide (OSO): a theoretical study, J. Chem. Theor. Comput. 7 (2011) 2104–2111.

[16] (a) Y. Lan, K.N. Houk, Mechanism and stereoselectivity of the stepwise 1,3-dipolar cycloadditions between a thiocarbonyl ylide and electron-deficient dipolarophiles: a computational investigation, J. Am. Chem. Soc. 132 (2010)

17921–17927;
(b) C. Di Valentin, M. Freccero, R. Gandolfi, A. Rastelli, Concerted vs stepwise mechanism in 1,3-dipolar cycloaddition of nitrone to ethene, cyclobutadiene, and benzocyclobutadiene. A computational study, J. Org. Chem. 65 (2000) 6112–6120;
(c) R.A. Firestone, Mechanism of 1,3-dipolar cycloadditions, J. Org. Chem. 33 (1968) 2285–2290.

[17] (a) A. Sengupta, B. Li, D. Svatunek, F. Liu, K.N. Houk, Cycloaddition reactivities analyzed by energy decomposition analyses and the frontier molecular orbital model, Acc. Chem. Res. 55 (2022) 2467–2479;
(b) M.S.T. Morin, D.J. St-Cyr, B.A. Arndtsen, E.H. Krenske, K.N. Houk, Modular mesoionics: understanding and controlling regioselectivity in 1,3-dipolar cycloadditions of münchnone derivatives, J. Am. Chem. Soc. 135 (2013) 17349–17358;
(c) L. Xu, C.E. Doubleday, K.N. Houk, Dynamics of 1,3-dipolar cycloaddition reactions of diazonium betaines to acetylene and ethylene: bending vibrations facilitate reaction, Angew. Chem. Int. Ed. 48 (2009) 2746–2748;
(d) D.H. Ess, K.N. Houk, Distortion/interaction energy control of 1,3-dipolar cycloaddition reactivity, J. Am. Chem. Soc. 129 (2007) 10646–10647;
(e) D.H. Ess, K.N. Houk, Theory of 1,3-dipolar cycloadditions: distortion/interaction and frontier molecular orbital models, J. Am. Chem. Soc. 130 (2008) 10187–10198;
(f) D.H. Ess, K.N. Houk, Activation energies of pericyclic reactions: performance of DFT, MP2, and CBS-QB3 methods for the prediction of activation barriers and reaction energetics of 1,3-dipolar cycloadditions, and revised activation enthalpies for a standard set of hydrocarbon pericyclic reactions, J. Phys. Chem. A 109 (2005) 9542–9553.

[18] (a) Z. Benke, M. Nonn, F. Fülöp, L. Kiss, An insight into selective olefin bond functionalization of cyclodienes through nitrile oxide 1,3-dipolar cycloadditions, ChemistrySelect 4 (2019) 2886–2891;
(b) Z. Benke, M. Nonn, A.M. Remete, S. Fustero, L. Kiss, Diversity-oriented synthesis of highly functionalized alicycles across dipolar cycloaddition/metathesis reaction, Synlett 32 (2021) 1911–1933.

[19] (a) Z. Benke, A.M. Remete, A. Semghouli, L. Kiss, Selective functionalization of norbornadiene through nitrile oxide cycloaddition/ring-opening/cross-metathesis protocols, Asian J. Org. Chem. 10 (2021) 1184–1191;
(b) L. Kiss, M. Nonn, F. Fülöp, Syntheses of isoxazoline-based amino acids by cycloaddition of nitrile oxides and their conversion into highly functionalized bioactive amino acid derivatives, Synthesis 44 (2012) 1951–1963.

[20] Gaussian 16, Revision B.01, Frisch, M. J.; Trucks, G. W.; Schlegel, H. B.; Scuseria, G. E.; Robb, M. A.; Cheeseman, J. R.; Scalmani, G.; Barone, V.; Petersson, G. A.; Nakatsuji, H.; Li, X.; Caricato, M.; Marenich, A. V.; Bloino, J.; Janesko, B. G.; Gomperts, R.; Mennucci, B.; Hratchian, H. P.; Ortiz, J. V.; Izmaylov, A. F.; Sonnenberg, J. L.; Williams-Young, D.; Ding, F.; Lipparini, F.; Egidi, F.; Goings, J.; Peng, B.; Petrone, A.; Henderson, T.; Ranasinghe, D.; Zakrzewski, V. G.; Gao, J.; Rega, N.; Zheng, G.; Liang, W.; Hada, M.; Ehara, M.; Toyota, K.; Fukuda, R.; Hasegawa, J.; Ishida, M.; Nakajima, T.; Honda, Y.; Kitao, O.; Nakai, H.; Vreven, T.; Throssell, K.; Montgomery, J. A., Jr.; Peralta, J. E.; Ogliaro, F.; Bearpark, M. J.; Heyd, J. J.; Brothers, E. N.; Kudin, K. N.; Staroverov, V. N.; Keith, T. A.; Kobayashi, R.; Normand, J.; Raghavachari, K.; Rendell, A. P.; Burant, J. C.; Iyengar, S. S.; Tomasi, J.; Cossi, M.; Millam, J. M.; Klene, M.; Adamo, C.; Cammi, R.; Ochterski, J. W.; Martin, R. L.; Morokuma, K.; Farkas, O.; Foresman, J. B.; Fox, D. J. Gaussian, Inc., Wallingford CT, 2016.

[21] A.V. Marenich, C.J. Cramer, D.G. Truhlar, Universal solvation model based on solute electron density and on a continuum model of the solvent defined by the bulk dielectric constant and atomic surface tensions, J. Phys. Chem. B 113 (2009) 6378–6396.

[22] Stationary points related to the step-by-step mechanism were not found when performing the DFT calculations, both in vacuum and in a simulated solvent (acetonitrile), supporting then, that the reaction proceeds via the proposed concerted mechanism.

[23] (a) T. Hansen, P. Vermeeren, F.M. Bickelhaupt, T.A. Hamlin, Origin of the α-effect in S_N2 reactions, Angew. Chem. Int. Ed. 60 (2021) 20840–20848;
(b) T. Hansen, P. Vermeeren, A. Haim, M.J.H. van Dorp, J.D.C. Codée, F.M. Bickelhaupt, T.A. Hamlin, Regioselectivity of epoxide ring-openings via S_N2 reactions under basic and acidic conditions, Eur. J. Org. Chem. 2020 (2020) 3822–3828.

[24] (a) P. Vermeeren, T. Hansen, M. Grasser, D. Rodrigues Silva, T.A. Hamlin, F.M. Bickelhaupt, S_N2 versus E2 competition of F– and PH_2^- revisited, J. Org. Chem. 85 (2020) 14087–14093;
(b) P. Vermeeren, T. Hansen, P. Jansen, M. Swart, T.A. Hamlin, F.M. Bickelhaupt, A unified framework for understanding nucleophilicity and protophilicity in the S_N2/E2 competition, Chem. Eur J. 26 (2020) 15538–15548;
(c) D.E. Ortega, R. Ormazábal-Toledo, R. Contreras, R.A. Matute, Theoretical insights into the E1cB/E2 mechanistic dichotomy of elimination reactions, Org. Biomol. Chem. 17 (2019) 9874–9882.

[25] (a) P. García-Aznar, J. Escorihuela, Computational insights into the inverse electron-demand diels–alder reaction of norbornenes with 1,2,4,5-tetrazines: norbornene substituents' effects on the reaction rate, Org. Biomol. Chem. 20 (2022) 6400–6412;
(b) J. Escorihuela, W.J.E. Looijen, X. Wang, A.J.A. Aquino, H. Lischka, H. Zuilhof, Cycloaddition of strained cyclic alkenes and *ortho*-quinones: a distortion/interaction analysis, J. Org. Chem. 85 (2020) 13557–13566;
(c) D. Svatunek, R.P. Pemberton, J.L. Mackey, P. Liu, K.N. Houk, Concerted [4 + 2] and stepwise (2 + 2) cycloadditions of tetrafluoroethylene with butadiene: DFT and DLPNO-UCCSD(T) explorations, J. Org. Chem. 85 (2020) 3858–3864;
(d) T.A. Hamlin, D. Svatunek, S. Yu, L. Ridder, I. Infante, L. Visscher, F.M. Bickelhaupt, Elucidating the trends in reactivity of aza-1,3-dipolar cycloadditions, Eur. J. Org. Chem. 2019 (2019) 378–386;
(e) T.A. Hamlin, B.J. Levandowski, A.K. Narsaria, K.N. Houk, F.M. Bickelhaupt, Structural distortion of cycloalkynes influences cycloaddition rates both by strain and interaction energies, Chem. Eur J. 25 (2019) 6342–6348;
(f) D. Gahtory, R. Sen, A.R. Kuzmyn, J. Escorihuela, H. Zuilhof, Strain-promoted cycloaddition of cyclopropenes with o-quinones: a rapid click reaction, Angew. Chem. Int. Ed. 57 (2018) 10118–10122;
(g) J. Escorihuela, A. Das, W.J.E. Looijen, F.L. van Delft, A.J.A. Aquino, H. Lischka, H. Zuilhof, Kinetics of the strain-promoted oxidation-controlled cycloalkyne-1,2-quinone cycloaddition: experimental and theoretical studies, J. Org. Chem. 83 (2018) 244–252;
(h) B.J. Levandowski, K.N. Houk, Theoretical analysis of reactivity patterns in diels–alder reactions of cyclopentadiene, cyclohexadiene, and cycloheptadiene with symmetrical and unsymmetrical dienophiles, J. Org. Chem. 80 (2015) 3530–3537.

[26] (a) J.A. Escorihuela, Density functional theory study on the cobalt-mediated intramolecular pauson–khand reaction of enynes containing a vinyl fluoride moiety, Synthesis 55 (2023) 1139–1149;
(b) J. Escorihuela, L.M. Wolf, Computational study on the Co-mediated intramolecular pauson–khand reaction of fluorinated and chiral *N*-tethered 1,7-enynes, Organometallics 41 (2022) 2525–2534;
(c) J.J. Cabrera-Trujillo, I. Fernández, Factors controlling the aluminum(I)-meta-Selective C–H activation in arenes, Chem. Eur J. 27 (2021) 12422–12429;
(d) P. Vermeeren, T.A. Hamlin, I. Fernández, F.M. Bickelhaupt, Origin of rate enhancement and asynchronicity in iminium catalyzed diels–alder reactions, Chem. Sci. 11 (2020) 8105–8112;
(e) T. Sergeieva, T.A. Hamlin, S. Okovytyy, B. Breit, F.M. Bickelhaupt, Ligand-Mediated regioselective rhodium-catalyzed benzotriazole–allene coupling: mechanistic exploration and quantum chemical analysis, Chem. Eur J. 26 (2020) 2342–2348;
(f) G. Casella, C. Fonseca Guerra, S. Carlottoe, P. Sgarbossaf, R. Bertanif, M. Casarin, New light on an old debate: does the RCN–$PtCl_2$ bond include any back-donation? RCN←$PtCl_2$ backbonding vs. the IR νC≡N blue-shift dichotomy in organonitriles–platinum(II) complexes. A thorough density functional theory – energy decomposition analysis study, Dalton Trans. 48 (2019) 12974–12985.

[27] B. Lin, P. Yu, C.Q. He, K.N. Houk, Origins of regioselectivity in 1,3-dipolar cycloadditions of nitrile oxides with alkynylboronates, Bioorg. Med. Chem. 24 (2016) 4787–4790.

[28] C. Gonzalez, H.B. Schlegel, Reaction path following in mass-weighted internal coordinates, J. Phys. Chem. 94 (1990) 5523–5527.